中華民國六十八年九月十一日～十二日

第一屆中華民國電子顯微鏡學會
學術研討會摘要

THE FIRST R.O.C. SYMPOSIUM ON ELECTRON MICROSCOPY

ABSTRACT

September 11-12, 1979

Chang Gung Memorial Hopital
Linkou Medical Center
Taipei, Taiwan, Republic of China

長庚林口醫學中心

The First R.O.C. Symposium on Electron Microscope Sponsered by The Cardiovascular Division of Chang Gung Memorial Hospital

Organizing Committee

President:

Y.S. Lee, MD, FCCP
李英雄
Chief of Cardiovascular Division

Secretary General:

Y.T. Sung, MD, MRCP
宋銀子

Members:

J. Chen, J.B. Hsu, T.P. Huang
陳 中 許如璧 黃子平

H.Y. P'eng, K.L. P'eng, J.H. Tsao
彭惠玉 彭凱玲

Scientific Exhibition and Abstract:

Y.Y. Chou, SC(ASCP), MT(ASCP) and T.P. Huang
周雲英 黃子平

With the Assistance of the Committee of Electron Microscopy of Chinese Society of Materials Science

The Committee of Electron Microscopy

President:

Y.L. Chen
陳衍隆　國立工業技術學院機械系

Vice-President:

S.S. Lee
李英雄　長庚紀念醫院心臟血管內科

Members:

S.T. Chang
張順太　中國鋼鐵公司研究發展處

L.J. Chen
陳力俊　清華大學材料科學工程研究所

M.J. Chen
陳脈紀　中興大學植物病理學系

T.H. Hsu
許廷珪　金屬工業研究所

K.S. Lu
盧國賢　台灣大學醫學院解剖學系

L.P. Lin
林良平　台灣大學農學院農化系

S.M. Liang
梁序穆　國防醫學院生物形態學學系

W.S. Wang
王文雄　台灣大學機械系

Programme for Physical Science

Schedule on 11th September

8:30-9:00AM --- Registration
9:00-9:50AM --- Opening Ceremony 一樓生化講堂

9:50-10:10AM --- Tea Time

Special Lecture:

Coordinator: 陳衍隆

10:10-11:50AM --- Electron Microscopy in Materials Sciences ---------- 1
Prof. Gareth Thomas

12:00AM-13:00PM --- Lunch

Session I: High Strength Steels 高強度鋼

Coordinator: 陳衍隆

13:10-13:40PM --- A Study of the Microstructure of 250 Maraging Steel Weldment --------- 3
楊春欽 陳衍隆 鮑亦當

13:40-14:10PM --- Retained Austenite and Tempered Martensite Embrittlement of Fe-Mn-C Steels ---------- 4
王建義 陳衍隆 王文雄

14:10-14:40PM --- A Study of Nichel-Containing Maraging Steel and Manganess-Containing Maraging Steel ---------- 5
侯天益 王文雄 陳衍隆

14:40-15:10PM --- Electron Diffraction Patterns: Cementile vs. Chi-carbide ---------- 6
馬哲保

15:10-15:30PM --- Tea time

15:30-16:00PM --- The Fractographic Investigations of Low-Stress Fracture by Scanning Electron Microscopy ---------- 7
陳弘毅 載萍平 楊春欽 端木蕙

Session II: Crystallization and Defects 結晶及晶格缺陷

Coordinator: 陳力俊

16:00-16:30PM --- Application of Electron Microscopy to the Study of $CuInS_2$ Layers ------ 8
黃惠良 鄭祝良 曾百亨

16:30-17:00PM --- Investigation of Microstructural Defects in Ion-Implanted Silicon ---- 10
陳力俊 吳逸蔚 王紀中 施義成

17:00-17:30PM --- Crystallization of Amorphous Silicon in Si/Al/Si Film ---------- 11
焦一虹 馬哲申 周安琪

Scientific Programme for Medical Biological Science

Schedule on 12th September

Special Lecture

Coordinator: 梁序穆　林槐三

9:00-10:40AM --- High Voltage Electron Microscopy in Biology ---------- 43
Prof. Kiyoshi Hama

10:40-11:00AM --- Tea time

Session III: Medical Science

Coordinator: 李英雄

11:00-11:15AM --- A Review of the Ultrastructural Changes in Myocardial Disease of Various Etiologies ---------- 44
李英雄

11:15-11:30AM --- Morphometric Electron Microscopic Studies of Cardiac Hypertrophy-using Different Experimental Models -- 47
宋銀子

11:30-11:45AM --- Glomerular Microfibrils in Renal Disease ---------- 49
許輝吉

11:45-12:00AM --- The Ultracytochemical Study of GERL in Hepatoma Ascites Cells ------ 50
王長君

12:00AM-13:00PM --- Lunch

13:00-14:30PM --- Organic Disease Visualized as Structural Defects of the Cell by Means of SEM
Prof. Lenuart Nilsson, Dr. Ruland

14:30-15:00PM --- 200 KV High Resolution Electron Microscope and its Application
Yoshio Noguchi

15:00-16:30PM --- Ultramicrotomy 1979, Techniques and Instrumentation
Norma Reid

Schedule on 12th September

Special Lecture

Coordinator: 陳衍隆

9:00-10-40AM --- Direct Observation of Atoms in Molecules and Crystal and Electron Micro-Cinematographic Study of Dynamic Behaviour of Atoms ---------- 12
Prof. H. Hashimoto

10:40-11:00AM --- Tea time

Session III: Thermomechanical Treatment 熱機處理

Coordinator: 陳力俊

11:00-11:30AM --- Microstructures Associated with Optimal Mechanical Properties for a Thermomechanical Treated 1050 Plain Carbon Steel ---------- 14
陳力俊 鄭見忠 吳才偉

11:30-12:00AM --- The Effects of Rolling on Precipitates of Al-Zn-Mg Alloy ---------- 16
劉國維 雷啓元 洪健龍

12:00AM-13:00PM --- Lunch

13:00-13:30PM --- The Thermal Mechanical Studies of Brass ---------- 17
萬其明 江銘添 周海邦

13:30-14:00PM --- The Application of SEM to the Study of Fatigue Initiation in Pure Aluminium ---------- 18
江銘添 林 燦 萬其明

14:00-14:30PM --- Tea time

14:30-15:00PM --- 200 KV High Resolution Electron Microscope and its Application
Yoshio Noguchi 一樓生化講堂

15:00-16:30PM --- Ultramicrotomy 1979, Techniques and Instrumentation
Norma Reid 一樓生化講堂

Programme for Medical Biological Science

Schedule on 11th September

8:30-9:00AM --- Registration
9:00-9:50AM --- Opening

9:50-10:10AM --- Tea time

Special Lecture

Coordinator: 林槐三　梁序穆

10:10-11:50AM --- The Fine Structure of Photoreceptive Membrane as Revealed by Electron Microscopy
Prof. Eichi Yamada ---------- 19

12:00AM-13:00PM --- Lunch

Session I: Medical Science

Coordinator: 林槐三

13:10-13:25PM --- Some Observations on the Fine Structure of the Pineal of the Black Rat (Rattus rattus) in the Natural Habitat ---------- 20
黃宏圖

13:25-13:40PM --- Some Observation on the Fine Structure of the Pineal Stalk in the Golden Hamster ---------- 21
曾國藩　林槐三

13:40-13:55PM --- Effect of Sympathetic Ganglionectomy on the Cholinesterase Activity of the Hamster Pineal Gland --------- 23
張丙龍

13:55-14:10PM --- Effect of Thyroidectomy and Propyl Thiouracil on the Fine Structure of the Golden Hamster ---------- 25
王淑美　林槐三

14:10-14:25PM ---cUltrastructural and Cytochemical Studies on the Hamster Subcommissural Organ ---------- 27
盧國賢

14:25-14:40PM --- Mitochondrial Inclusions in the Renal Epithelial Cells of the Rat of Long-Evans Strain ---------- 29
廖克剛

14:40-14:55PM --- The Neuroglial Reactions in the Cuneate Nucleus Ager after Dorsal Rhigotomy ---------- 30
溫振源

Electron Microscopy in Materials Sciences

Gareth Thomas

Professor, Department of Materials Science and Mineral Engineering, College of Engineering, and Materials and Molecular Research Division,
Lawrence Berkeley Laboratory, University of California,
Berkeley, California 94720

Abstract

The properties of materials are structure-sensitive. Structure is in turn determined by composition, heat-treatment, and processing. Thus, it is necessary to characterize both composition and microstructure at highest levels of resolution possible in order to understand materials behaviour. Such characterization requires advanced and sophisticated methods of analysis using microscopic, diffraction, and spectroscopic techniques. For this, of course. electron microscopy is particularly versatile, since we are now routinely synthesizing structure almost at atomic levels of resolution. The interaction between composition, heat treatment, and properties is complex, but this interaction must be understood if materials are to be improved or new materials to be designed.

Considerable developments in electron microscopy have occurred in the last decade, notably those in high-resolution microscopy, especially at higher voltages (See Fig. 1), and in microanalytical techniques using TEM/STEM with X-ray or electron energy loss (Table 1). These permit the Materials Scientist to make considerable progress in understanding materials behavior.

In this paper examples will be given for a range of materials problems (e.g. steels, Fig. 2 and ceramics, Fig 3).

Table I. Chemical Analysis Methods by Electron Microscopy

Method	Spatial (Å)	Spectroscopic Resolution (atomic fraction)	Lattice Parameter (%)
STEM X-ray	-50[a]	10^{-5} (Z 11)	-
STEM energy spectroscopy	-50-5000[b]	10^{-2}	-
Lattice imaging	-2	-	-0.5 (real space)
Microdiffraction	-20	-	-1 (real space)
Converging beam	-50	-	-0.1 (Kikuchi)
Critical voltage	-100	10^{-2}	

[a]Although smaller spot sizes are possible, the signal-to-noise ratio determines the optimum.

[b]Modern developments suggest that 50 Å will be possible (limited by source brightness and signal detection).

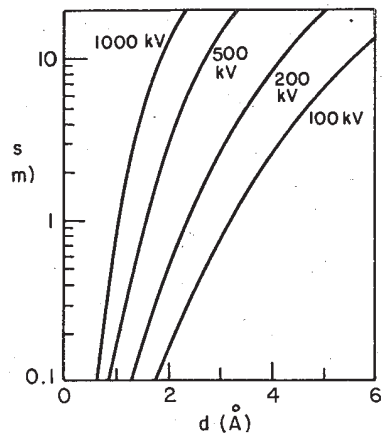

Fig. 1-Resolution vs. Voltage and Spherical Aberration

Fig. 2-Dark field image of HSLA steel, quenched from 1100°C showing retained austenite and carbides.

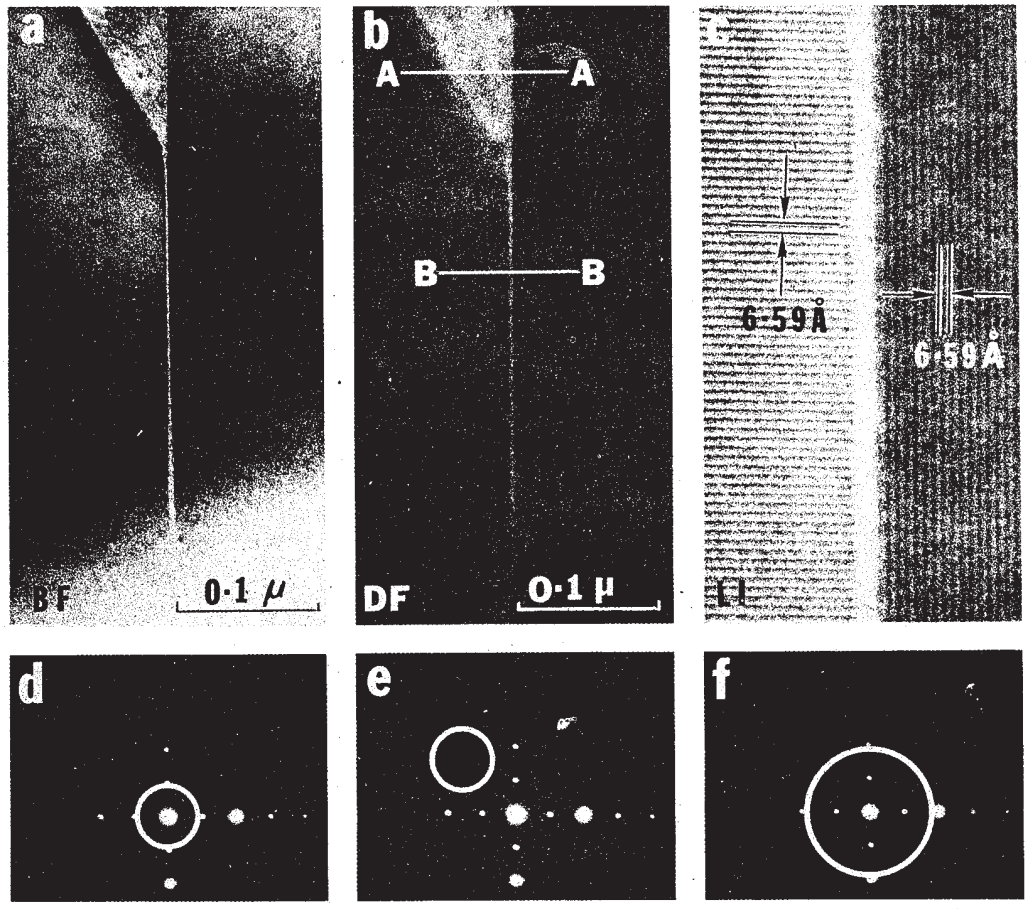

Fig. 3-Bright field, dark field, and lattice imaging of Si_3N_4 showing glassy phase at grain boundaries: EDAX analysis shows Ca in the glass.

A Study of the Microstructure of 250 Maraging Steel Weldment

C.C. Young*, Y.L. Chen**, Y.T. Pao**

楊春欽　陳衍隆　鮑亦當

* Chun-Shan Institute of Science and Technology

** Department of Mechanical Engineering and Technology

National Yaiwan Institute of Technology

Abstract

One of the purposes of this research is to correlate the mechanical properties with the microstructure of 250 maraging steel weldments. The strengthening precipitates were identified as Ni_3Mo and O-FeTi by using trans-mission electron microscopy. The dark-etched region in the HAZ and the cellualr or dendritic structures in the fusion zone are two weaker regions of the TIC weldments of this alloy due to overaging and the existence of reverted austenite. The SEM+ EDAX microsegregation in the fusion zone. It was found that at cell boundaries and in the interdendritic regions it was enriched in Ti, Mo and Ni.

Retained Austenite and Tempered Martensite Embrittlement of Fe-Mn-C Steel

J.Y. Wang*, Y.L. Chen** and W.H. Wang*

王建義　陳衍隆　王文雄

* Department of Mechanical Engineering, National Taiwan University

** Department of Mechanical Engineering and Technology
National Taiwan Institute of Technology

Abstract

In the investigation of Fe-Mn-C steels, there are small amounts of very finely despersed films of retained austenite which can be resolved at the interface between martensite laths in the as-quenched state. Upon tempering at 350°C thermal instability causes austenite films to decompose at the lath boundaries to form cementite which are probably responsible for the embrittlement.

A Study of Nickel-Containing Maraging Steel and Manganess-Containing Maraging Steel

T.Y. Hou*, W.H. Wang* and Y.L. Chen**
侯天益　王文雄　陳衍隆

* Department of Mechanical Engineering, National Taiwan University

** Department of Mechanical Engineering & Technology
National Taiwan Institute of Technology

Abstract

Two kinds of maraging steels were melted under the protection of Argon atmosphere in this experiment. One is 17.9Ni-8.5Co-4.7Mo-0.5Ti designated as T-alloy, the other is 13Mn-8.6Co-4.6Mo designated as M-alloy. T-alloy was heated at 820°C for one hour, cooled in the air, and then aged at 430°C, 480°C, 530°C. M-alloy was heated at 850°C for one hour refrigerated in liquid nitrogen for 3 hours, and then aged at 430°C, 480°C, 530°C.

The results show that aging at 480°C for 15 hours the hardness of T-alloy reached a maximum (Hv 508) with tensile strength 170kg/mm^2 yield strength 162kg/mm^2, elongation 5% and impact value 2.7kg-m/cm^2. For M-alloy, aging at 530°C for 2 hours, an optimal combination of mechanical properties can be attained: tensile strength 155kg/mm^2, yield strength 124kg/mm^2, elongation 8.5% and impact value 1.7kg-m/cm^2. TEM shows that the strengthening precipitates of T-alloy include Ni_3Mo, Ni_3Ti, and σ-FeMo.

Application of Electron Microscopy to the Study of $CuInS_2$ Layers

H.L. Hwang*, C.L. Cheng** and B.H. Tseng**
黃惠良　鄭祝良　曾百亨
* Dept. of Electrical and Power Engineering
** Dept. of Material Science and Engineering
National Tsing Hua University
Hsin-Chu, Taiwan, R. O. C.

Abstract

In recent years, the I-III-VI_2 tenary chalcopyrite compounds have found increasing interest in semiconductor science. Mainly due to its direct gap (1.55eV) $CuInS_2$ could be used in high efficiency solar cells. In this work, $CuInS_2$ layers were prepared by

1. RF sputtering
2. Chemical vapour transport

Single phase $CuInS_2$ powders were synthesized and used for the material preparation, and in sputtering pressed disks were used as the target. In RF sputtering, the Ar pressure was kept between 20-40 microns, and the RF frequency was kept between 12 to 14 MHZ. There was no substrate heating, and the deposition rate was about 1200Å/hr. The as-deposited films on slide-glasses were verified to be single phase $CuInS_2$ by T.E.D., and from which the preferred orientation could not be observed.

The grain size is smaller than 1000Å, which were calculated from the line broadening of the X-ray diffraction patterns and further checked by T.E.M.

Epitaxial $CuInS_2$ layers have been grown on (111) GaP substrates via chemical vapour transport, which were done in a single zone furnace. The charge end was kept in the range of

780°C, while the substrate was held at 640°C. The iodine amount was about 1-1.5mg/cc. The transport was done in 29 hours.

The electron micrograph (SEM) showed triangular pyramids of the epi-grown $CuInS_2$ layers on GaP (111) A-plane, and hexagonal pyramids on GaP (111) B-plane. The as-grown layers were determined to be single crystalline with (112) orientation by back reflection laue method.

Investigation of Microstructural Defects in Ion-Implanted Silicon

L.J. Chen, I.W. Wu, J.J. Wang and Y.C. Shih
陳力俊　吳逸蔚　王紀中　施義成
Dept. of Materials Science and Engineering
National Tsing Hua University
Hsin-Chu, Taiwan, R. O. C.

Abstract

Transmission electron microscopy (TEM) has been applied to study the microstructural defects produced in post-implantation annealed silicon wafers. (111), and (001) silicon samples were irradiated by 100 KeV BF_2^+, P^+ and As^+ to doses 5×10^{13} to 1×10^{16} cm^{-2} followed by isothermal annealing in dry N_2 from 600°C to 1200°C for ½ hr to 4 hr.

Disordered zones, rod-like defects, Frank loops, perfect dislocation loops, half-loops, stacking fault, dislocation lines, twins as well as dislocation networks were investigated by diffraction contrast methods. Particular examples are given in details to illustrate the application of TEM to the characterization of microstructural defects. Sheet resistivity measurements were made to correlate the electrical properties with microstructures.

Crystallization of Amorphous Silicon in Si/Al/Si Films

Yi-Hung Chiao, Jer-Shen Maa, An-Chich Chou
焦一虹　　馬哲申　　周安琪
Department of Materials Science and Engineering
National Tsing Hua University
Hsin-Chu, Taiwan, R. O. C.

Abstract

Low temperature ($100^{\circ}C \sim 400^{\circ}C$) crystallization phenomena of electron beam evaporated Si films in the self-supporting sandwhich films of Si-Al-Si have been studied by means of transmission electron microscopy. Depending on the thickness of aluminum layer, the transformation of metastable amorphous Si films into crystalline structure may proceed by different reactions such as polymorphous transformation into supersaturated crystalline solid solution or eutectic decomposition or direct crystallization on the grain boundaries of Al layer. The crystallization temperature and crystal size of Si films are also affected by the thickness of Al film.

Direct Observation of Atoms in Molecules and Crystals and Electron Micro-cinematographic Study of Dynamic Behaviour of Atoms

Prof. H. Hashimoto
Osaka University
Faculty of Engineering
Department of Applied Physics
Suita, Osaka 565, Japan

Abstract

1. Fine structure of the images of atoms in crystals

It was demonstrated by the present authors[1,2,3] that inner fine structure of the images of atoms in gold crystal in 100 orientation could be photographed by 100 KV electron microscopes adjusted at "aberration free focus(AFF)" condition. In the present observation, similar fine structures have been observed in the images of atoms in gold crystal in 110 orientation.

These fine structures correspond to the flux distribution of electron waves passing through the potential field in atoms and show that incident electrons behave, as quantum mechanical particles, like the electrons originally belonging to atoms.

11. Atomic arrangement around stacking faults, twins and their intersections

Atomic arrangement around an intrinsic and extrinsic stacking fault in gold thin single crystal whose surface is parallel to (110) plane has been observed. Intersection of two intrinsic faults produces a sessile dislocation with the reaction of two partial dislocations at the end of the faults[4]. Some examples have been observed, one of which seems to be

produced by the reaction.

$$a/6(2\bar{1}\bar{1}) + a/6(\bar{2}1\bar{1}) = a/3(00\bar{1})$$

In some case no sessile dislocation is ovserved, which suggests that the Burgers vectors of the partial dislocations at the ends of two intersecting faults do not form an energetically stable dislocation and actually the faults soon separated.

III. Dynamic behaviour of atoms in the twin formation

Dynamic process of the formation and disappearance of twin is recorded as TV images. One intrinsic stacking fault plate is developed from the surface of the crystal in the first step and then another intrinsic fault is formed along the developed intrinsic fault, which produces the extrinsic fault (one atom twin plate). The fault plate was formed within 0.07 seconds. The rearrangement of atoms at the tip of the twin plate is also recorded as TV images. Twin plates cometimes have small miorientation. Dynamic behaviour of atoms at the tip of twin plate will be shown in a movie film.

IV. Dynamic behaviour of Th atoms forming ThO_2 crystals.

By electron irradiation, thorium atoms in thorium piromeritate molecules which are supported on graphite thin film form thouium oxide crystals. Movement and growth process of atoms are recorded as TV images. Movement of atoms at intervals of 0.08 sec. is seen. Dynamic behaviour of atoms will be shown in a movie film.

1) H. Hashimoto et al : J. Phys. Soc. Japan 42, 1073 (1977).
2) H. Hashimoto and H. Endoh : Electron Diffraction (50th Anniversary) London, 64, (1978).
3) H. Hashimoto et al. : 0th International Congress of Electron Microscopy, Totonto, 3, 244 (1978).
4) A.H. Cottrell : Phil. Mag., 43, 645 (1952)

Microstructures Associated with Optimal Mechanical Properties for a Thermomechanically Treated 1050 Plain Carbon Steel

L.J. Chen, H.C. Cheng and T.W. Wu
陳力俊　鄭見忠　吳才偉

Department of Materials Science and Engineering
National Tsing Hua University
Hsin-Chu, Taiwan, R.O.C.

Abstract

A study of the microstructure and mechanical properties of thermomechanically treated 1050 carbon steel has been carried out by optical metallography, scanning and transmission electron microscopy, tensile as well as hardness tests. The steels were first transformed to two distinct structures, i.e. fine and course pearlites. These samples were reduced 75% in thickness by cold rolling, then heat treated at 780°C (up-quenching) or 650°C (annealing) for different periods of time, followed by air-cooling. The mechanical properties were found to be vastly improved by the suitable thermomechanical treatments. A significant improvement in yield strength was accompanied by moderate changes in ultimate tensile strength and elongation.

Two kinds of distinct microstructures were found to be associated with improvements in mechanical properties.

(1) subgrains confined between partially spheroidized lamellar cementite in pearlite regions. The confinement of subgrains by cementite increased the strength, where as the spheroidization of cementite was beneficial in obtaining good ductility.

(2) fine subgrains (or grains) about 1 μm in diameter and dispersed globular carbide particles. The marked improvements in mechanical properties may be attributed to the grain refinement effect, substructure and dispersion strengthenings.

The Effect of Rolling on Precipitates of an Al-Zn-Mg Alloy

K.S. Liu, C.Y. Lei and J.L. Horng
劉國維 雷啓元 洪健龍
Department of Materials Science and Engineering
National Tsing Hua University
Hsin-Chu, Taiwan, R. O. C.

Abstract

An assessment is conducted on the use of TEM observation, resistivity, hardness and size-distribution curve to study the effect of rolling after different preaging treatments on precipitation and dislocation structure of an Al-6%Zn-1%Mg alloy. The processes are THA and TAHA, which in later case chosen with 2 hours and 5 days preaging at 100°C, all final aging treatments are at 100°C and 135°C. The aim of the paper is to examine the effect on phase change of precipitates under different preaging and working treatments. There is show good mechanical performances when we suitably control the preaging temperature and time in the TMT process. The relationships between preaging treatments and the morphology of precipates after 135°C final aging have been found. Besides, we find that long rod-like η precipitates broken after rolling and their shapes changed during the final aging at 135°C.

The Thermal Mechanical Studies of Brass

C.M. Wan, M.T. Jahn and H.P. Chou
萬其明　江銘添　周海邦
Department of Materials Science and Engineering
National Tsing Hua University
Hsin-Chu, Taiwan, R. O. C.

Abstract

Microstructures studies of 70/30 and 90/10 brasses are performed with different levels of cold work, under different annealing temperatures and times.

Tensile properties are studied and correlated to the interior microstructures investigated after treatments for both alloys.

The Application of SEM to the Study of Fatigue Initiation in Pure Aluminium

M.T. Jahn, Tsann Lin and C.M. Wan
江銘添　林　燦　萬其明
Department of Materials Science and Engineering
National Tsing Hua University

Abstract

The effect of pre-existing subgrains on the fatigue initiation mechanism in pure aluminium has been studied by scanning electron microscopy. Various sizes (2∼4μ) of pre-existing subgrains are formed by low temperature thermomechanical treatment. The improvement of fatigue properties of the specimens containing pre-existing subgrains over those of the specimens either fully annealed or not fully polygonized will be discussed from the following respects: the degree of slip activity, the number of activated slip systems, the stress gradient at grain boundary and the fraction of subcells and subgrains after fatigue.

The Fine Structure of Photoreceptive Membrane as Revealed by Electron Microscopy

Prof. Eichi Yamada
Department of Anatomy
Faculty of Medicine
University of Tokyo

Abstract

The photoreceptive pigment molecules are usually localized in the biological membranes. For example, visiula pigments of vertebrate retina localize in the disk membrane within the outer segments of rod and cone, and of invertabrate retina in the rhabdomeric microvilli membranes. In the Halobacterium halobium, the bacteriorhodopsin molecule forms socalled purple membrane as a portion of bacterial plasma membrane. The study was focused on the ultrastructure of these membranes utilizing various techniques of electron microscopy. Particularly, the freeze-fracture replica method was extensively used, including deep etching on the unfixed materials.

The observations showed that these photoreceptive molecules were revealed as membrane particles on the P face of freeze-fractured membrane. In the cases of crayfish and squid retinas, the membrane particles showed a parallel arrangement along the axes of rhabdomeric microvilli. The arrangement suggests the effective sensitivity to the polarized light in these animals. Furthermore, the morphological aspect of visual pigment recycling or regeneration was recognized. In the purple membrane, the membrane particles were 50-60 Å in diameter and were closely packed, hexagonally arranged. Each particle appeared to be composed of three subunits which might correspond to the trimer of bacteriorhodopsin molecule.

Some Observations on the Fine Structure of the Pineal of the Black Rat (Rattus rattus) in the Natural Habitat

H.T. Huang
黃宏圖
Departments of Anatomy College of Medicine, National Taiwan University and Kao-hsiung Medical College

Abstract

Pineal glands of adult black rats, captured at the beginning of February in the rice, peanut and sweet potato fields of southern Taiwan, were studied with routine electron microscopy.

The perikaryon of the pinealocyte displays an indented nucleus with sparse heterochromatin and a prominent nucleolus, moderately developed Golgi apparatus, abundant round- and oval-shaped mitochondria, free polysomes and cisternae of granular and smooth endoplasmic reticula which situate in the cytoplasm between the mitochondria. Occasionally, small stacks of cisternae of granular endoplasmic reticulum are found.

The capillaries in the pineal are fenestrated. The perivascular spaces are well-developed, including a large number of non-myelinated nerve fibers and pinealocyte process endings. The pinealocyte process endings contain many dense cored and clear vesicles and grumose inclusions (Wolfe, 1965). The nerve fibers, some of which group into bundles invested by Schwann cells and some are free endings on the pinealocytes, are distinguishable by the presence of clusters of granulated vesicles of 40-60 nm in diameter.

Some Observations on the Fine Structure of the Pineal Stalk in the Golden Hamster

Guo-Fang Tseng and Huai-San Lin
曾國藩　　林槐三
Department of Anayomy, College of Medicine,
National Taiwan University
Taipei, Taiwan, R. O. C.

Abstract

In the golden hamster the pineal stalk extends from the superficial pineal gland located under the confluence sinus to the deep pineal attached to the habenular commissure. It is located under the suprapineal recess of the third ventricle, and bilaterally accompanied by veins which drain into the confluence sinus. The suprapineal recess is lined by epithelial cells of the choroid type with numerous microvilli and occasional cilia.

The stalk is formed by a number of fascicles of elongated cytoplasmic processes of pinealocytes and nerve fibers, which are invested by septal cells resembling the leptomeningeal cells located beneath the choroid epithelium. The central segment of the stalk attached to the deep pineal consists of 2 to 3 small fascicles containing many nerve fibers, mostly unmyelinated, and slender pinealocytic processes. Blood vessels are not incorporated in the fascicles of the central segment. Approaching to the superficial pineal, the stalk progressively gains its thickness as a result of increasing number of additional fascicles and blood capillaries. Nevertheless, nerve fibers are reduced in number, i.e., inversely proportional

to the predominance of thick pinealocytic processes. One to two weeks after removal of both superior cervical ganglia most of the nerve fibers in the deep and middle segments of the stalk remained intact, which suggests their origin other than the ganglia.

Effect of Sympathetic Ganglionectomy on the Cholinesterase Activity in the Hamster Pineal Gland

Ping-Lung Chang
張 丙 龍
Department of Anayomy, College of Medicine
National Taiwan University
Taipei, Taiwan, R. O. C.

Abstract

By employing biochemical assay and histochemical enzyme techniques the effect of superior cervical ganglionectomy on the cholinesterase (ChE) activity in the hamster pineal glands was investigated. Biochemical assay indicates that the ChE activity in the adult hamster pineal glands is 7.05 (expressed in μ moles acetylcholine hydrolyzed per min per g of tissue). Two weeks after superior cervical ganglionectomy, about 22% of ChE is lost. Ultrastructurally, the acetylcholinesterase (AChE) activities are localized in the perinuclear space, Golgi complex, and smooth-surfaced endoplasmic reticulum of the pinealocytes, and in the intercellular space between the pinealocytes. Enzyme reaction product is also detected in the unmyelinated adrenergic nerve fibers and endings as well as the myelinated nerve fibers within the pineal glands. After superior cervical ganglionectomy, the unmyelinated adrenergic nerve fibers have been completely degenerated, while some AChE are remained in the pinealocytes suggesting that these cells are able to produce AChE. Based on the present investigations together with those of the previous data, it is concluded that the unmyelinated adrenergic nerve fibers in the pineal glands are derived from the superior cervical ganglia, some of the acetylcholine and AChE are transmitted from the superior cervical ganglia via the postganglionic sympathetic adrenergic nerve fibers into the pineal glands, and then taken up by the pinealocytes; and that the increased weight of the testis in

the hamster following ganglionectomy is mainly due to the decreased pineal melatonin, which is caused by the decreased norepinephrine, acetylcholine and hydroxyindole-O-methyl transferase (HIOMT) in the pineal gland resulted in the destruction of the adrenergic nerve fibers within the pineal gland.

Effects of Thyroidectomy and Propyl Thiouracil on the Fine Structure of the Adenohypophysis of the Golden Hamster

Seu-Mei Wang, Huai-San Lin

王淑美　　林槐三

Department of Anatomy, College of Medicine,
National Taiwan University
Taipei, Taiwan, R. O. C.

Abstract

Anterior pituitaries from male hamsters which were either thyroidectomized or administered with propyl thiouracil (PTU), were studied along with those from untreated control animals. Specimens were processed by the conventional electron microscopic technique and by the periodic acid silver methenamine reaction (PASM), a preferential stain for glycoproteins.

Our previous studies have morphologically distinguished six cell types in the anterior pituitary of the hamster. Among them T cells possess secretory granules of the smallest size and stainable with PASM, and were shown to be insignificantly affected by castration.

Four weeks after either thyroidectomy or PTU administration T cells appeared greatly stimulated to display well developed organelles indicative of high synthetic activity, and were predominated in the gland. Thus, T cells are considered to be TSH producing cells.

F cells, which do not contain secretory granules, were also particularly affected by these treatments. Glycogen particles and fat droplets accumulated in the cytoplasm of most F cells. Frequently follicles were found composed of peculiar F cells, the cytoplasm of which was extensively expand-

ed by an enormous glycogen pool. The peculiar F cells seldom occur in the gland under normal or other experimental conditions such as castration and adrenalectomy.

Ultrastructural and Cytochemical Studies on the Hamster Subcommissural Organ

Kuo-Shyan Lu
盧國賢
Department of Anatomy, College of Medicine,
National Taiwan University,
Taipei, Taiwan, R. O. C.

Abstract

Conventional electron microscopy has failed to reveal any formed structures, such as dilated cisternae of the endoplasmic reticulum, corresponding to the secretory granules in the hamster subcommissural organ (SCO) cells. Otherwise, the ultrastructure of the hamster SCO cells is essentially similar to that of the other species, i.e., the slender SCO cells, in which the free surface is provided with numerous microvilli and one or two cilia, possess highly indented nuclei, abundant mitochondria, well developed Golgi apparatus with associated vesicles and dense bodies, and a great amount of cytoplasmic filaments and microtubules.

After staining with periodic acid silver methenamine (PASM) techniques (Rambourg, 1967, J. Cell Biol. 15, 409-412), a rather homogeneous but weakly-stained background over all the cytoplasm was observed and no structures suspected to be the secretory granules were identified. Two or three inner Golgi saccules and numerous dense bodies were also specifically stained.

Acid phosphatase activity was prominent and mainly located in a very complicate anastomosing tubules in the inner aspect of the Golgi apparatus. Dense bodies also show

the acid phosphatase activity and they were regarded as lysosomes.

Since there is no conviencing evidence indicating the presence of the formed secretory granules in the hamster SCO cells, we suggest that the secretory material are probably glycoprotein in nature and may exist in a soluble form. Furthermore, we speculate that Golgi apparatus is responsible for the formation of lysosomes and might be involved in the elaboration of the secretory material as well.

Mitochondrial Inclusions in the Renal Epithelial Cells of the Rat of Long-Evans Strain

Ko Kaung Liao
廖克剛
Departments of Anatomy, Chung Shan Medical and Dental College, and College of Medicine, National Taiwan University

Abstract

Intramitochondrial inclusions have frequently been observed in the cells of the uriniferous tubules, especially of the thick distal tubules in rats of Long-Evans strain. Two types of filamentous bodies occur in the mitochondrial matrix: one is composed of a bundle of 5 nm thick filaments, the other consists of similar filaments with regular light and dark bands of about 30 nm periodicity.

Microcylinders, which were first described in the mitochondria of pinealocytes of Long-Evans rats, have been frequently encountered in the renal epithelial cells. They are located within the cristae, and less frequently, in the space between the inner and outer mitochondrial membranes. Each of microcylinders is composed of one central and six peripheral filamentous subunits. Another inclusions found in the cristae are helical filaments similar to those observed in astrocytes of albino rats. In some instances continuations of helical filaments with the subunit filaments of microcylinders can been seen. The observations suggest that the subunit filaments of the microcylinders are formed by tightly wound helical filaments.

The Neurogilial Reactions in the Cuneate Nucleus after Dorsal Rhizotomy

Chen-Yuan Wen
溫振源
Department of Anatomy, College of Medicine
National Taiwan University

Abstract

The processes of the neuroglial elements clearly showed reactive changes caused by the experimental degeneration. The most obvious sign was phagocytic glial hyperplasia. The number of processes containing bundles of filaments was markedly increased when compared with the control. The processes of the phagocytic glial cells were seen to surround the degenerating elements. Some glial cells showing mitotic division were also noted in the 3 and 4 days' survival material. The number of glial cells was greatly increased, particularly the phagocytic glial cells which were more often seen than in normal animals. Their appearance suggested increased activity. The volume of their cytoplasm was greatly increased and invariably different stages of phagosomes. Some engulfed degenerating axon terminals characterized by swollen mitochondria or synaptic vesicles could still be identified. In a few instances, a clear profile resembling an electron-lucent type of degenerating axon terminals has been observed within the cytoplasm of a phagocytic glial cell. Only swollen mitochondria but not synaptic vesicles or other organelles were present. The oligodendrocytes, however, did not show any definite reactive changes.

Electron Microscopic Study of Foamy Virus Particles.

Wu-Tse Liu
劉武哲
Department of Microbiology, National Yang-Ming Medical College, Shih-pai, Taipei 112, Taiwan, R. O. C.

Abstract

In this study, the morphology of chimpanzee foamy virus particles was examined by electron microscopy. Thin-sections of human and rabbit kidney, rat embryo and WI-38 cells revealed similar viral morphology. Two categories of virus-like particles were observed: small, ring-shaped particles (nucleoids) 30-50 nm in diameter, with an electron-lucent center and an electron-dense shell; and large, mature of complete virions measuring 100-140 nm in diameter including the outer shell and spikes of 10-15 nm.

The naked nucleoids were seen as clusters or singly in the cytoplasmic matrix; no viral structures were seen in the nucleus of stationary or dividing cells. The mature virions usually appeared to arise from buddings of the nucleoids from the plasma membranes, membranes of cytoplasmic vacuoles and of Golgi complex. In this budding process the external envelope and spikes were acquired. This process was usually multiple, involving the production of several virions at one site. With negative staining, it was possible to show the morphology of extracellular virions. With this method, they were measured 110-125 nm with a nucleoid of 70-80 nm. Pleomorphism was great both with negative staining and in thin sections.

A Morphological Approach of the Tarsonemid Mite *Steneotarsonemus Spinki* Smiley (Tarsonemidae) as a Rice Plant Pest

Y.S. Chow, S.S. Tzean, C.S. Chang and
C.H. Wang
周延鑫
Institute of Zoology, Academia Sinica Taipei
115, Taiwan R. O. C.

Abstract

Results obtained from a study of mouthparts and the digestive system of *Steneotarsonemus spinki* Smiley by using scanning and transmission electron microscopy and physiological staining techniques prove it as an important pest of rice plants. The cheliceral stylet of the mite can puncture the soft surface or epidermis of the rice plant and suck the juices. When the mite population is large in the paddy field, it can also transmit sheath rot disease of rice. In the second crop season of Taiwan, heavy sterility of rice plants is possibly due to the large spread of this mite. Light and transmission electron micrographs of the mite's degestive system are also shown.

Index descriptors (in addition to those in title): Ultrastructure, *Acrocylindrium oryzae* Sawada and *Spiroplasm citri*.

*This research was supported by the National Science Council NSC-67B-0201-03(27) Taipei, Taiwan. R. O. C.

Observations on the Mature Ovule of *Cymbidium Ensifolium*

Yang-Chu Shiao, Yung-Reui Chen
蕭揚區　　陳榮鋭
Department of Botany
National Taiwan University
Taipei, Taiwan, R. O. C.

Abstract

Self-pollinated cymbidiums were used as materials in this experiment. Ovule maturation was observed about 120 days after pollination. Both the inner and the outer integuments consisted of 2 to 3 layers of cells showing prominent cell organelles, e.g., mitochondria, plastids, endoplasmic reticulum and plasmodesmata. Amorphous mucilage occurring outside the outer integument was often observed. Hypostase found near the chalazal end of the embryo sac constituted a group of thick-walled cells containing a nucleus and little cytoplasm. The pollen tube entering the micropyle has two sperm nuclei and one vegetative nucleus. During the fertilization, the pollen tube penetrated the filiform apparatus of the embryo sac and ejected the pollen discharges into the central cell. Both the embryo sac and pollen tube contained many oil droplets, but only the pollen tube had starch grains. The degenerated nucellus stained darkly and appeared in areas near the embryo sac.

A Study of the Fine Structural Changes in Post-Harvested Asparagus Spears during the Toughening Process

C.Y. Hsia, Doris C.N. Chang
夏鎮洋　　張喜寧

Department of Horticulture
National Taiwan University
Taipei, Taiwan, R. O. C.

Abstract

Transmission and scanning electron microscopic techniques were applied to study the fine structural changes in post-harvested asparagus spears during the toughening process.

The results showed that the freshly harvested white asparagus was already well lignified in the perivascular fiber ring portion, while the green asparagus was still almost non-lignified. With increase of storage days, progressively more cell lignification occurred in both perivascular fiber ring and vascular bundles, and it ultimately extended throughout the whole spear. Most of these changes could be clearly revealed 3-dimentionaly by the SEM.

Transmission electron micrographs showed that in green asparagus, the structural changes mainly ocurred in the thickening of cell walls, and the rupturing of chloroplast and mitochondrial double membranes. In general, white asparagus spears became thougher much more rapidly than the green spears, mainly due to the rapid thickening and increase in lignification of the cell walls.

SEM Observations of Cycas Revoluta

C.Y. Hsia, S.J. Chiou, Doris C.N. Chang
夏鎮洋　邱素貞　張喜寧
Department of Horticulture Na
National Taiwan University
Taipei, Taiwan, R. O. C.

Abstract

Cycas revoluta is one of the most striking ornamentals of tropical and subtropical area. Its beautiful golden sporophyll and dark shining green leaves are quite astonishing in the gardens. In this study, we observed these organs and spores of Cycas revoluta through SEM. More details have been revealed to support further research on this plants are of great importance to ornamental horticulture.

A SEM Study of Vasicules and Arbuscules Formation by Glomus sp. Mycorrhizal Fungus in Rangpur Lime Roots

R.S. Huang, C.Y. Hsia and Doris C.N. Chang
黃瑞祥　夏鎮洋　張喜寧
Department of Horticulture
National Taiwan University
Taipei, Taiwan, R. O. C.

Abstract

Mycorrhizal fungi are known to be beneficial to many plants. In our preliminary tests, we observed these beneficial effects of Glomus sp. on citrus through different cultural media tests. This report is a SEM study on the relationship between this fungus and Rangpur Lime roots. Along with the penetration of the fungus, both vasicular and arbuscular structures are found in the citrus roots. Among these structures, vasicules are known to be the storage organ of the fungus, but arbuscules though formed by the fungus are main structures that are thought to be beneficial to plants. When arbuscules are formed in the host cell, starch grains of these cells disappear, and finally these structures will be digested and consumed by the host cell, thus the mycorrhizal fungi are also known as one kind of 'biotic fertilizer'.

Disease Cycle of Rice Blast Caused by Pyricularia Oryzae Cav.

Hsin-Kan Wu
吳信淦
Institute of Botany
Acadawia Sinica
Taipei, Taiwan, R. O. C.

Abstract

Pyricularia oryzae is an imperfect fungus. Most strains are mononucleated. Conidia germinate on the rice leaves at temperature around 25°C. Appressoria often appear soon after germination.

Penetration takes place through epidermis cells and/or stoma of the leaves or of the panicle neck. The mycelium then spreads toward various directions into neighbour cells. No hostorium has been observed. After a short incubation period (3 or 4 days), the fungus comes out mostly through lower epidermis (in the case of leaf blast) and produces conidiophores and conidia. The mycellia which had invaded into the vascular bundles grows longitudinally and more rapidly than that in other parenchyma cells. Thus, it enlarges the lesion and makes the lesion spindle shaped. Such lesions produce numerous conidiophores and conidia over a period of several days.

The host parenchyma cells in the infected area dry out and/or have their organellae disintegrated so that the leaf blade becomes disorganized and thinner in the central part of the lesion.

Evidences showed that hyphal asastomoses have occurred in the naturally infected lesion.

Electron Microscopy of Cultivated Green Algae Chlorella Pyrenoidosa

S.W. Huang*, V.C. Liao**, H.C. Chen**, L.P. Lin**
黃書瑋　廖文基　陳琇青　林良平
* Southern-Asia College, Tauyuang, Taiwan
** Department of Agricultural Chemistry, National Taiwan University

Abstract

Photosynthetic unicellular algae can be cultivated by employing mass production techniques. Algal cells are harvested and spray-dried into dry powder. Under the observation of SEM each particle of this dry powder, consists of a few thousands cells. The impurities of cells were attached on the surface of cells. We have also performed concurrent ultrastructural analyses which permit the correlation of metabolic activities with quantitative stereological estimates of the volumes of cellular organelles and with the progress of structural changes.

Under heterotrophic growth, C. Pyrenoidosa formed autospores in the mature cell. These autospores were released by rupturing the mother cell wall. This strain accumulated many starch granules, and reduced thylakoid number in chloroplast. The structure of pyrenoid also diminished under heterotrophic conditions. Being transfered into autotrophic conditions, the cells recovered their thylakoid number and pyrenoid structure, and starch granules were reduced.

Studies on the Rice Protoplasts-Ultrastructural Changes during Enzymatic Isolation

Kwan-Long Lai and Li-Fei Liu
賴光隆　　劉麗飛
Department of Agriculture
National Taiwan University

Abstract

This paper reports the effect of digesting enzymes and hypertonic saline on ultrastructural changes of protoplasts isolated from etiolated rice plant.

A 7-days old aseptic rice (Oryza sativa L. cv Taichung Native No.1) shoot part was used for protoplasts isolation. The materials were put in 10ml enzyme sol. containing 2% cellulase, 1% macerozyme (Onozuka R-10), 2% KCl and 1% $MgSo_4$ in a 50ml Erlenmeyer flask. The PH value was 5.8.The enzyme sol. was sterilized by a 0.45μM millipore filter. The materials in the enzyme sol. was incubated in the dark for 6 hr. at 28°C for protoplast isolation. After filtration and centrifugation, the protoplasts were then suspended in 0.6M mannitol solution, the suspension was mixed with an equal volume of the mannitol sol. containing 1.2% agar, and solidified in room temperature. For comparison, the shoot materials untreated with enzyme sol., the shoots immersed in 2% KCl and 1%$MgSO_4$ sol. for 6 hr. only were also used. The shoot materials and the $1mm^3$ agar block containing isolated protoplasts, were fixed with 2% glutaraldehyde in 0.2M cacodylate buffer, PH 7.2, for 1 hr. and kept over-night in the refrigerator and then post fixed in 2% osmium tetroxide in above buffer for 2 hr. at 4°C, and dehydrated, embedded in epoxy resin. The thin sections were stained with uranyl acetate and

lead citrate, and observed with Hitachi HU-12 electron microscopy with 75K accelerating voltage. The results of the experiment were summarized as following: Most of the isolated rice protoplasts exhibited structural integrity. No structural remnants of cell wall could be seen, and the plasmalemma became the boundary of protoplasts containing nucleus, proplastids, mitochondria, endoplasmic reticulum, Golgi bodies, and numerous small vesicles. However, various degrees of structural changes were noted in a portion of isolated protoplasts. The most striking changes were found in mitochondria and proplastids. Occasionally, seriously damaged nuclei could be found in deformed protoplasts. Besides, plasmodesmata also proceeded morphological changes under enzyme treated condition. The somewhat swollen proplastids with protruded membranes in outer regions had swollen stroma lamella, large space and a row of small space on the margin. We found a kind of large crystalline inclusion bodies in cytoplasm of rice protoplast instead of in proplastid as reported by Fowke et al(1977) in soybean cell culture and pea leaf protoplast. In general, inclusion bodies were regarded as a storage form of protein. In the mitochondria, the number of cristae was apparently reduced, only very few cristae were arranged on the periphery leaving large portion of transparent area with their filaments.

In order to understand whether the above mentioned structural changes were caused by enzymatic digestion or simply by osmotic stress, we carefully reexamined the ultrastructures of shoots treated with enzyme in saline solution and shoot treated with saline only. The phenomena under electron microscopy clearly showed that these structural changes could induced by osmotic stress of saline, since the abnormal appearances of mi-

tochondria and proplastids were easily found in juvenile leaf tissues which were plasmolysed with saline only.

lead citrate, and observed with Hitachi HU-12 electron microscopy with 75K accelerating voltage. The results of the experiment were summarized as following: Most of the isolated rice protoplasts exhibited structural integrity. No structural remnants of cell wall could be seen, and the plasmalemma became the boundary of protoplasts containing nucleus, proplastids, mitochondria, endoplasmic reticulum, Golgi bodies, and numerous small vesicles. However, various degrees of structural changes were noted in a portion of isolated protoplasts. The most striking changes were found in mitochondria and proplastids. Occasionally, seriously damaged nuclei could be found in deformed protoplasts. Besides, plasmodesmata also proceeded morphological changes under enzyme treated condition. The somewhat swollen proplastids with protruded membranes in outer regions had swollen stroma lamella, large space and a row of small space on the margin. We found a kind of large crystalline inclusion bodies in cytoplasm of rice protoplast instead of in proplastid as reported by Fowke et al(1977) in soybean cell culture and pea leaf protoplast. In general, inclusion bodies were regarded as a storage form of protein. In the mitochondria, the number of cristae was apparently reduced, only very few cristae were arranged on the periphery leaving large portion of transparent area with their filaments.

In order to understand whether the above mentioned structural changes were caused by enzymatic digestion or simply by osmotic stress, we carefully reexamined the ultrastructures of shoots treated with enzyme in saline solution and shoot treated with saline only. The phenomena under electron microscopy clearly showed that these structural changes could induced by osmotic stress of saline, since the abnormal appearances of mi-

tochondria and proplastids were easily found in juvenile leaf tissues which were plasmolysed with saline only.

Protein Inclusions in Elongating Stipes of *Agaricus Bisporus*

Liang-Ping Lin
林良平
Department of Agricultural Chemistry
National Taiwan University

Abstract

Ultrastructural features of cells in stipe portions of fruit-bodies are described. Stipe samples of fruit-bodies were harvested at three different elongation stages. membrane complexes are evident in the cells. Extensive occurences of vesicles and vacuoles in the elongating cells of stipes were observed. The insoluble protein is concentrated towards the top of the stipes, but the upper parts of the stipe showed the greatest decline in insoluble protein during the stipe expansion.

The prominent features of all stages of stipe development in *A. bisporus* are large membrane-bounded protein inclusions with flattened faces. Just before opening of pileus these inclusions appear to reach their maximum size and completely filling the enclosing membrane. Protein inclusion possessed a crystalline substructure. Attempts to quantify the distribution of protein inclusions using electron microscopy were unsuccessful but chemical analysis gave the patterns. Appearence and quantitative changes of protein inclusions suggested that such inclusions participitate in cell expansion during the fruit-bodies development.

High Voltage Electron Microscope in Biology

Prof. K. Hama M.D.
The Institue of Medical Science
The University of Tokyo

Abstract

The major advantages of the application of high voltage electron microscopy in the field of biology are

1. higher penetrating power of electrons which enables the observation of the thicker specimen
2. lower beam damage to the specimen
3. higher resolution

The first and second properties are especially useful in the biological research. At 1,000 KV, epon section of over 5 μm thick can be observed with reasonable resolution. Utilizing this property, the three dimensional organization of neurons and glia cells in the central nervous system was observed. The detail of the branching pattern of neuronal and glial processes was first analyzed by high voltage electron microscopy of Golgi impregnated material.

The exposure time for the electron microscope autoradiography could be reduced remarkably by using the thick specimen. Some examples of this field will also be presented.

At 800 KV, the beam damage to the specimen was estimated to be about one third of that at 75 KV. This property together with the first one, the higher penetrating power of electrons, opened the possibility of observing the biological material at the more native state. The observation of hydrated biological specimen using an environmental cell will be presented.

A Review of the Ultrastructural Changes in Myocardial Diseases of Various Etiologies

Ying-Shiung Lee M.D.
李 英 雄
Cardiovascular Division,
Department of Internal Medicine,
Chang Gung Memorial Hospital

Abstract

Electron microscopic studies on the ultrastructural changes resulted from myocardial diseases of various etiologies were carried out in patients with congenital and rheumatic heart diseases. The specimens were obtained from the myocardium of the right or left ventricles. The tissues were fixed with 3% glutaraldehyde solution followed by 2% osmium tetroxide, and then stained with uranyl acetate and lead citrate. The ultrastructure of the myocardium was examined in the Hitachi H-500 scanning and transmission electron microscope operated at 75 KV. The ultrastructural changes were summaried in the following.

Degenerative changes of the myofibrils involved the myofilament and the Z-lines. Loss of myofilaments involved one or more sarcomeres. The Z-lines frequently showed structural changes of the shape and size including thickening, distortion and fragmentation of the Z-lines. A peculiar change referred to as streaming of the Z-lines was often observed. Target fibers which were related to streaming of the Z-lines were not infrequently seen in severe degenerative myocardium. These degenerative changes of the myofibrils were reflected in the configuration of the muscle fibers, the surface of which often became indented or presented sarcoplasmic projections. Disarray and loss of the myofibrils were accompanied

by changes in the shape and size of the muscle fibers.

Regarding the regeneration of the myofibrils, numerous fine filaments and well-formed myofibrils scattered throughout the sarcoplasm, particularly in the subsarcolemmal area.

The common changes of the mitochondria were marked variation in their number, size and shape. The mitochondrial cristae became less electron dense and underwent fragmentation and eventually disappeared. The intramitochondrial granules increased in number. Glycogen granules were noted to be accumulated in the mitochondria. Vesicles, vacuoles, tubular structures, membranes and myelin bodies appeared in the mitochondria.

The nuclei were often enlarged with peripheral condensation of the chromatin situated chiefly at the nuclear margin. One or more prominent nucleoli were often noted. Frequently the surface of the nuclei were indented. The Golgi apparatus often presented more flattened tubules with terminal expainsions.

The morphologics change of the longitudinal sarcoplasmic reticulum was unfolding and distention. The rough sarcoplasmic reticulum was more abundant. The transverse tubular system were particularly enlarged and expanded, which sometimes showed a honeycomb structure of varying size.

The glycogen was often increased and accumulated throughout the muscle fibers, but especially between the myofibrils and under the plasma membrane. Lipofuscin was often observed. Vacuoles and autophagic vacuoles of varying size as well as myelin and membranous bodies were often seen under the plasma membrane and between myofibrils.

The review illustrated the manifold ultrastructural changes of the human myocardium in heart diseases of various etiologies that might underlie myocardial failure. An attempt was made to correlate these morphologic changes to

functional impairment in heart muscle.

Morphometric Electron Microscopic Studies of Cardiac Hypertrophy --- Using Different Experimental Models

Y.T. Sung
宋 銀 子
Cardiovascular Division,
Department of Interanl Medicine,
Chang Gung Memorial Hospital

Abstract

Morphometric changes of cardiac hypertrophy and its regression have been studied using three different experimental models in the rat.

1. Left ventricular pressure overloading from constriction of the abdominal aorta;
2. Iron-deficiency anaemia;
3. Chronic isoprenaline administration.

Aortic banding in young (21 days) rats caused gradual constriction and led after 3 months to 53% hypertrophy which regressed to normal 11 days after removal of the band. Morphometry showed no changes in myofibrillar or mitochondrial size which reverted to normal 11 days after removing the band.

Iron deficiency (from 10 days of age) led after 35 days to 45% hypertrophy, which only partly regressed up to 43 days after giving iron. Morphometry showed no change in myofibrillar but an increase in mitochondrial volume density without change in size; these changes reverted to normal within 10 days.

Isoprenaline (5mg/Kg/day) given to adult rats for 10 days led to 52% hypertrophy, which regressed to normal 14 days later. Morphometry showed normal myofibrillar but reversibly increased mitochondrial volume density as in iron deficiency but here associated with an apparent decrease in mitochondrial size.

Mitochondrial numbers appeared to be increased in all three

models of comparably sever hypertrophy, though there was no measurable increase in mitochondrial volume denisty in the mechanical overload model.

Glomerular Microfibrils in Renal Diseases

Hcy-Chi Hsu, D.D.S., M.S.(Path),
許 輝 吉
Department of Pathology, College of Medicine,
National Taiwan University
Taipei, Taiwan, R. O. C.

Abstract

Small microfibrils of about 100 Å thick have been well defined in connective tissues in association with a variety of structures, but rarely described in the human glomerulus. In a previous report (Hsu HC, Suzuki Y, Grishman E, and Churg J:Kidney International, 1979, in press), a systematic study conducted on a comparative basis has demonstrated the existence of the glomerular microfibrils in the peripheral capillary walls in addition to the well-described mesangial areas. An ultrastructural similarity between these glomerular microfibrils and the connective tissue microfibrils is also demonstrated. The present report will summarize the occurrence of glomerular microfibrils in various renal diseases, including chronic renal allograft rejection. The glomerular microfibrils, when present in the peripheral capillary, are exculsively in the widened and usually lucent subendothelial aspect of the glomerular basement membrane (GBM). Evidence of gradual incorporation into the GBM is also demonstrated. The pathologic significance of the occurrence will be discussed.

The Ultracytochemical Study of GERL in Hepatoma Ascites Cells

J.J. Wang
王長君
Department of Biomorphics
National Defense Medical Center
P.O. Box 8244, Taipei, Taiwan R. O. C.

Abstract

Acid phosphatase (ACPase) and thiamine pyrophosphatase (TPPase) are the marker enzymes of lysosome and Golgi apparatus, seperately. They were used by many investigators for the demonstration of GERL area in different cell lines histochemically or cytochemically.

Both these cytochemical methods were used to define the GERL area of Chang hepatoma ascites cells in this report. The influence of dimethyl sulfoxide (DMSO) on ACPase reaction was included.

The results showed various reacting sites of ACPase on lysosomes and Golgi apparatus, and TPPase on Golgi apparatus will be discussed.

Medtronic

REICHERT JUNG

環宇光學有限公司

UNIVERSAL OPTICAL & INSTRUMENTS LTD.

電話：351-2059
P.O.BOX:59664

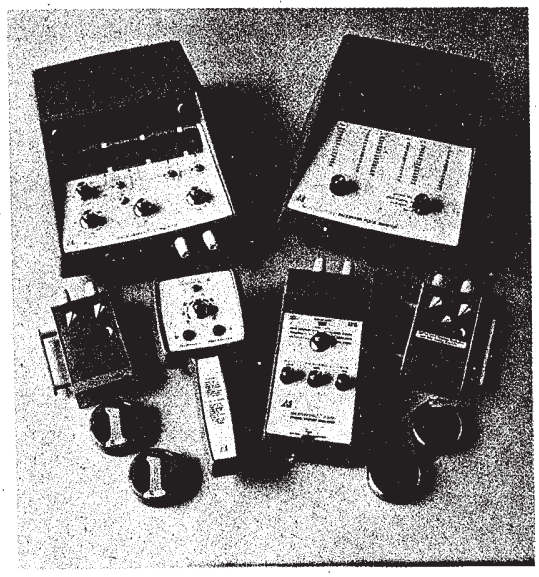

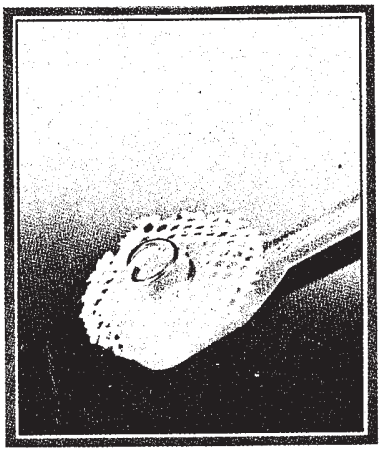

The Unique
Model 6917A
Sutureless Lead

- Permanent Pacemaker
- XYREL--Bipolar, Unipolar, Demand
- Lithium Pacemaker
- Demand Ventricular Programmable
- Demand Atrial Programmable
- Nuclear Pacemaker, Bipolar
- External Pacemaker
- Pacing System Analyzer
- Pacemaker Pulse Monitor
- Progammable Stimulator
- Temporory Pacing Lead

- Scanning Electron Microscope
- Laboratory Microscope
- Research Microscope
- Universal Microscope
- EM-Lab Instruments
- Ultramicrotome
- Rotary Microtome
- Sliding Microtome
- Freezing Microtome
- Scientific Instruments

JEOL

Resolution, penetration and less-damage... all these are neatly integrated in JEM-200C

Compact 200 kV JEM-200CX

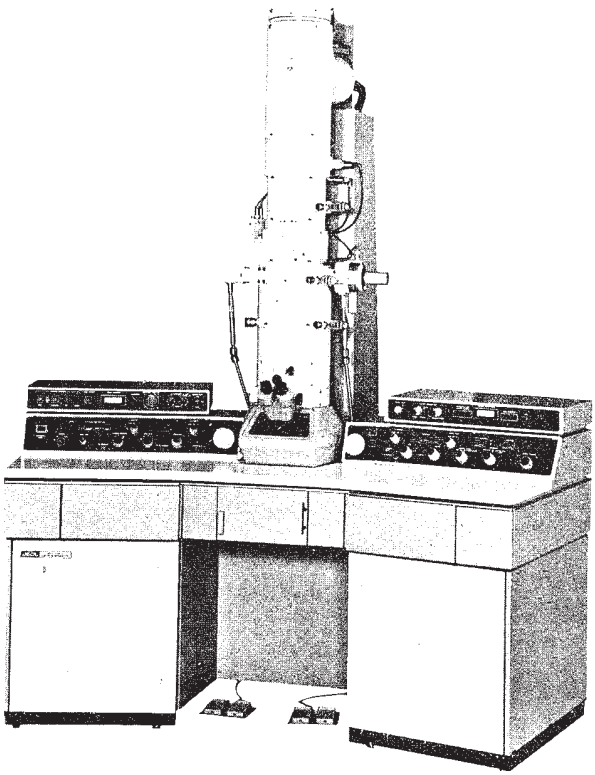

- A eucentric side entry goniometer with a 1.4 Å guaranteed resolution and ±30° tilt capability is provided as standard.
- The compact six-stage-acceleration electron gun allows easy and stable application of high voltage, and features simplicity of maintenance. A LaB_6 cathode is attachable as an option.
- Provides medium- and low-magnification images of high contrast and high quality.
- Provides a clean high vacuum of 10^{-7} Torr, reducing specimen contamination. A newly designed optional anticontamination device further reduces specimen contamination.
- The aberration-free, fully balanced deflector system (JEOL PAT.) permits the incident beam to be tilted ±4° in all directions, allowing a high-intensity dark field image to be obtained at the touch of a single button.
- Provided with the same operational conveniences as on the time-proven JEM-100CX, including the optimum focus control precentered filament, etc.
- As compact as a 100 kV electron microscope, requiring no special room for installation.
- Expandable to a 200 kV analytical electron microscope with a high resolution scanning device (ASID), energy dispersive X-ray spectrometer (EDS) and energy analyzer (ASEA).

JEOL LTD.

三光儀器股份有限公司
San Kwang Instruments Co., Ltd.
總公司：台北市永綏路２０號（中山堂正門前）
電話：(02) 3715171·3615446
台中營業所：台中市三民路１段１２５之２號
電話：(042) 282611
高雄營業所：高雄市大同一路１９５號
電話：(07) 2112186

a New Analytical Research TEM

技術的日立！服務的益弘！

HITACHI

MODEL
H-600

ELECTRON MICROSCOPE

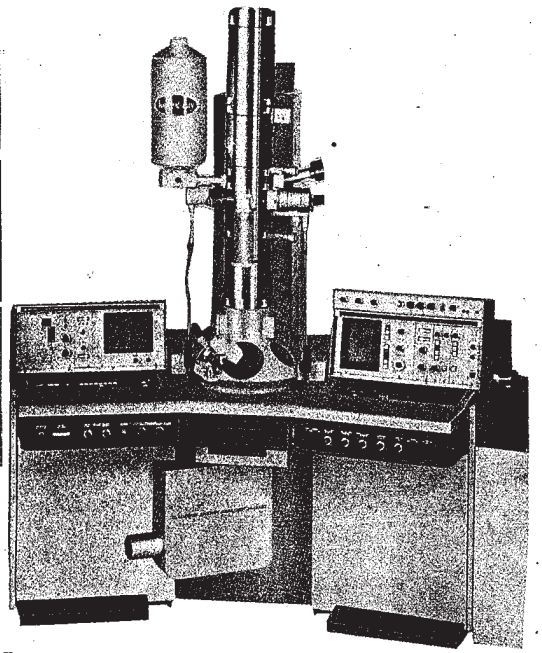

承蒙．長庚醫院……等
購買十八部電子顯微鏡，

特此致謝！

日立理化科學儀器產品：

各型電子顯微鏡	Electron Microscopes
高性能核磁共振儀	High Resolution NMR Spectrometer
紫外光—可視光分光光度計	UV-VIS Spectrophotometer
色度分析儀	Color Analyzer
紅外線分光光度計	Infrared Spectrophotometer
炎光光度計	Flame Spectrophotometer
原子分光光度計	Atomic Absorption/Flame Spectrophotometer
氣體層次分析儀	Gas Chromatograph
液體層次分析儀	Liquid Chromatograph
自動高速冷凍離心機	Automatic High Speed Refrigerated Centrifuges
螢光光度計	Fluorescence Spectrophotometer
自動氨基酸分析儀	Automatic Amino Acid Analyzer
氣相層析質譜儀	GC-MASS Spectrometer

日立理化科學儀器產品種類繁多，有關資料，歡迎來電洽詢。

日商日製產業株式會式

日立理化科學儀器

台灣總代理

益弘儀器股份有限公司

總 公 司：台北市松江路84巷4-1號　TEL: (02) 5311362-3　5311847　TELEX: 19702
高雄分公司：高雄市建國一路537號　TEL: (07) 2514121-2

Ladd SCIENTIFIC PRODUCTS FOR ELECTRON MICROSCOPY

LADD RESEARCH INDUSTRIES, INC.
P.O. BOX 901, BURLINGTON, VT. 05402
Area Code 802 • 658-4961
Telex 954644

ORDERING INFORMATION
All goods shipped F.O.B. Burlington, Vt. Terms: Net 30 days. Prices subject to change without notice

電子顯微鏡空的利器

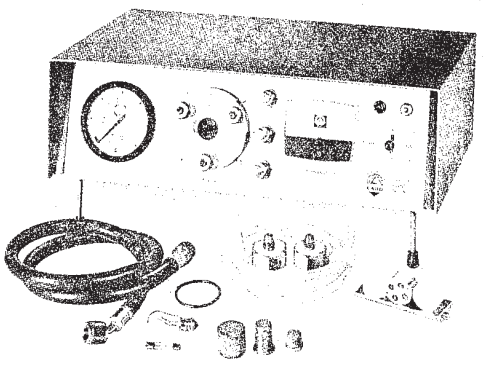

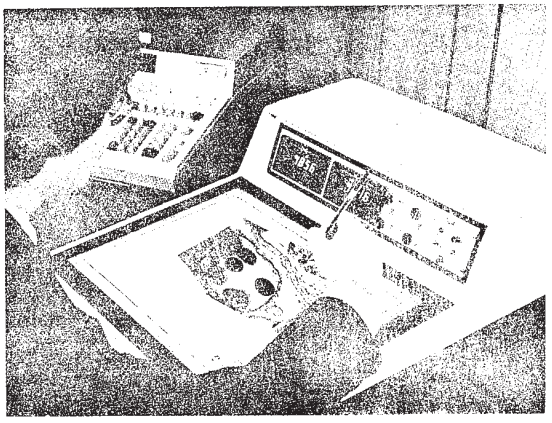

產品項目

VACUUM EVAPORATOR	CRITICAL POINT DRYER
FREEZE-FRACTURE U-NIT	DARKROOM ACCESSORIES
	EM-TISSUE PROCESSOR
GRAPHIC DATA ANALYZING SYSTEM	EMBEDDING KITS
	CHEMICALS & GRID

台灣總代理

UNION 友聖儀器有限公司
友聯光學公司

台北市忠孝東路三段251巷7弄4號
電話：7119427・7118447

興華儀器有限公司

SCHMIDT & CO.,(TAIWAN) LTD.

906 CHIA HSIN BUILDING, 96 CHUNG SHAN RD., NORTH SECT. 2, TAIPEI, TAIWAN.

台北市中山北路二段九十六號嘉新大樓九〇六室

TELEPHONE: 5515211 5318281 EXT. 481, 482

詳歡
細迎
資索
料取

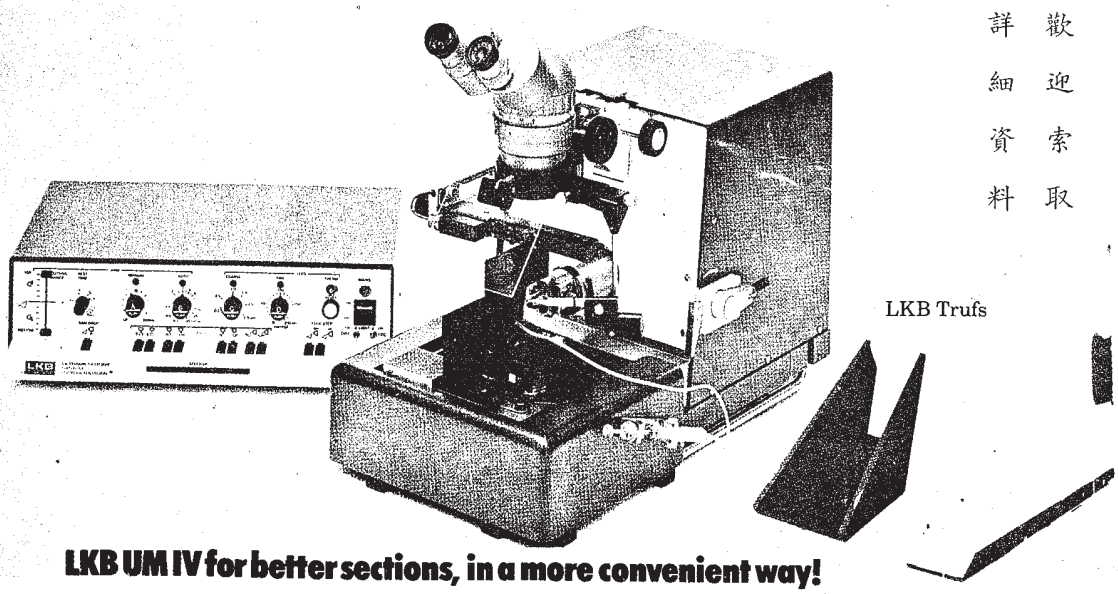

LKB Trufs

LKB UM IV for better sections, in a more convenient way!

The new LKB Ultrotome V Ultramicrotome

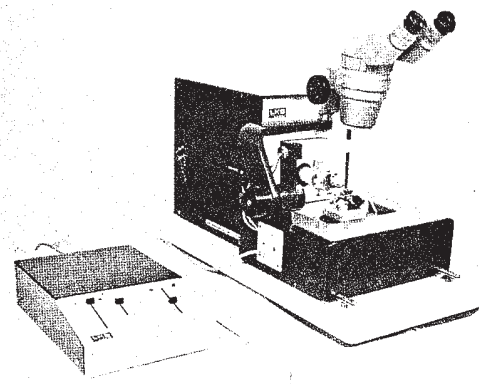

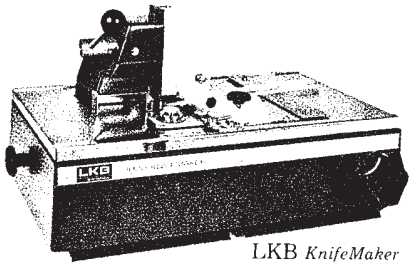

LKB *KnifeMaker*

KnifeMaker: perfect knives every time

New Disposable Knives for microtomy

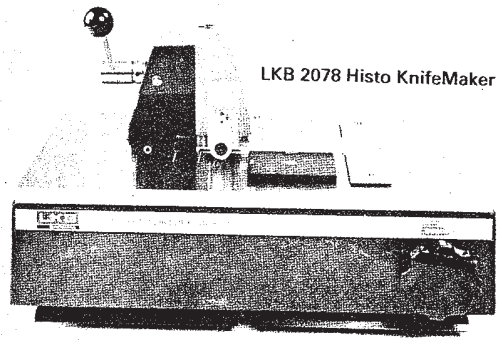

LKB 2078 Histo KnifeMaker

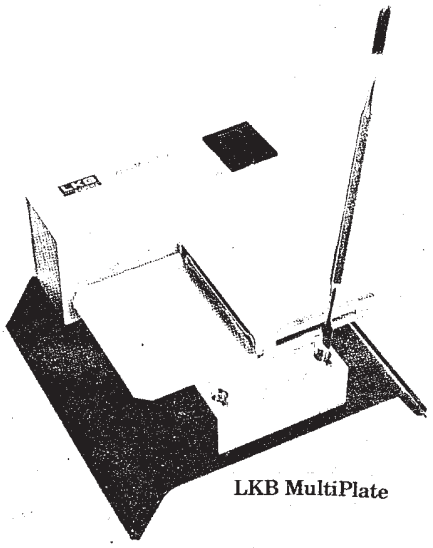

LKB MultiPlate

Myoglobin RIA

Insulin RIA

HPL RIA

ACTH RIA

Cyclic AMP RIA

Cortisol RIA

Aldosterone RIA

Angiotensin I RIA

Digoxin RIA

Cortisol RIA

The ways of saying quality

We represent the world's famous productions for: Radioimmunoassay Kits and Reagents.

Electron Microscopy Instruments, Acce..

NEN New England Nuclear

HYPOLAB

The Radiochemical Centre

BIODATA is the marketing organization for Serono

總代理: 全球化學藥品有限公司

Agent: **Universal Laboratory Chemicals Co., Ltd.**

258 Chin-Chou St. Taipei Taiwan Tel: 5116762, 5215405